Role of the Terminal Atoms in the Donor−Acceptor Complexes MX_3−D (M = Al, Ga, In; X = F, Cl, Br, I; D = YH_3, YX_3, X^-; Y = N, P, As)

Alexey Y. Timoshkin,*,† Andrew V. Suvorov,† Holger F. Bettinger,‡ and Henry F. Schaefer III‡

Contribution from the Department of Chemistry, Inorganic Chemistry Group, St. Petersburg State University, University Prospect 2, 198904, Old Peterhof, St. Petersburg, Russia, and Center for Computational Quantum Chemistry, University of Georgia, Athens, Georgia 30602-2556

Received September 24, 1998. Revised Manuscript Received February 17, 1999

Abstract: Donor−acceptor complexes MX_3−D (M = Al, Ga, In; X = F, Cl, Br, I; D = YH_3, PX_3, X^-; Y = N, P, As) and their components have been studied using self-consistent field and hybrid Hartree−Fock/density functional (B3LYP) methods with effective core potentials. The theoretical dissociation energies of the MX_3−D complexes decrease in the orders F > Cl > Br > I, Al > Ga < In, and N ≫ P ≥ As for all investigated complexes. The calculated (B3LYP/LANL2DZP) dissociation energies for ammonia adducts are on average 7 kJ mol^{-1} higher than those from experiment. There is *no correlation* between the dissociation energy and the degree of charge transfer. Complexes of ammonia and metal fluorides have mostly ionic metal−donor bonds, while the other donor−acceptor adducts are mostly covalently bonded. In addition, a significant charge redistribution between the terminal atoms leads to further electrostatic stabilization of ammonia adducts. Coulomb interactions destabilize MX_3−PX_3 complexes, and despite some experimental indications, the existence of these particular complexes in the gas phase is improbable. Distortion of MX_3 from planarity under complex formation leads to decreasing X−M−X angles. These decreasing angles correlate well with increasing M−X bond lengths. For all investigated MX_3−X^- systems a strong correlation of the MX_3−X^- dissociation energy with the M−X bond length increase is found. Correlations between the pyramidal angle X−M−Y and the length of the adjacent M−Y bond have been found for each donor atom Y. All observed trends in structural and thermodynamic properties are qualitatively explained on the basis of a simple electrostatic model.

Introduction

Complexes formed by Lewis acids and bases are widely known and of great importance in modern chemistry. One of the major characteristics of these adducts is the dissociation energy of the donor−acceptor bond, which can be derived from the energy of the complex formation in the gas phase. Mulliken proposed that donor−acceptor complex formation depends on the degree of charge transfer between the HOMO of the donor and the LUMO of the acceptor.[1] According to this point of view, the total charge-transfer q_{CT} from donor (D) to acceptor (A) should determine the energy of the donor−acceptor bond and, as a result, the dissociation energy (ΔH^{diss}). Indeed a linear correlation between q_{CT} and ΔH^{diss} has been observed for several classes of complexes.[2] However, in recent computational studies it has been shown that in some systems such a correlation is not valid.[3] This can be attributed to the importance of the terminal atoms in the complex formation.

The primary goal of this work is to investigate the role of the terminal atoms in the donor−acceptor complex formation of group 13 metal halides. Knowledge of the stability and thermodynamic characteristics of the adducts of the group 13 elements is essential for understanding the chemical vapor deposition of commercially important semiconductors, such as high-purity aluminum nitride and gallium arsenide.[4,5]

Neutral MX_3YH_3 adducts, formed by Al, Ga, and In halides with ammonia, phosphine, and arsine and ionic MX_4^- species were chosen for this investigation. Ammonia is a strong Lewis base, and its adducts have been widely investigated experimentally,[6] so direct experimental gas-phase data are available for comparison with our theoretical results. Phosphine and arsine are expected to be weaker donors; there are no experimental gas-phase data available on the formation energy of their complexes with MX_3.[7]

Despite many experimental and theoretical studies, the role of the terminal halogen atoms in complex formation is not fully understood. For boron halides the Lewis acid strength decreases in the order Br > Cl > F > I (according to experimental and ab initio data),[8] while for aluminum and gallium halides the orders F > Cl[9−11] and Br > Cl > I[6,12] were derived from theory and experiment, respectively.

* To whom correspondence should be addressed. E-mail: alex@dux.ru.
† St. Petersburg State University.
‡ University of Georgia.

(1) Mulliken, R. S.; Person, W. B. *Molecular Complexes*; Wiley: New York, 1969.
(2) Gurjanova, E. N.; Goldstein, I. P.; Romm, I. P. *Donor−Acceptor Bond*; Wiley: New York, 1975.
(3) Jonas, V.; Frenking, G.; Reetz, M. T. *J. Am. Chem. Soc.* **1994**, *116*, 8741.
(4) Lee, W. Y.; Lackey, W. J.; Agrawal, P. K. *J. Am. Ceram. Soc.* **1991**, *74*, 1821.
(5) Trachtman, M.; Beebe, S.; Bock, C. W. *J. Phys. Chem.* **1995**, *99*, 15028.
(6) Trusov, V. I. Ph.D. Thesis, Leningrad State University, 1974.
(7) Drago, R. S.; Joerg, S. *J. Am. Chem. Soc.* **1996**, *118*, 2654.
(8) Hirota, F.; Miyata, K.; Shibata, S. *J. Mol. Struct.: THEOCHEM* **1989**, *201*, 99.

10.1021/ja983408t CCC: $18.00
Published on Web 06/05/1999

The possible existence of donor−acceptor complexes in the gas phase mainly depends on the energy of the dative bond formed by the electron pair of the donor and the vacant orbital located on the acceptor.[13] While the dissociation enthalpy for strongly bonded adducts may be determined experimentally from vapor pressure studies, this method fails for adducts with a weak donor−acceptor bond. The investigation of these weakly bonded complexes in nonaqueous media leads to the inclusion of solvation effects, which can obscure the measured MX_3-D dissociation energy.

Complexes formed by Al, Ga, and In fluorides and ammonia have low volatility which precludes their investigation in the vapor phase. On the other hand, thermal destruction (pyrolysis) of iodide adducts starts at low temperatures, and the dissociation energy cannot be deduced from the experimental data obtained.[6] Usually thermodynamic, spectral, and structural data for adducts are obtained by different experimental methods and may have significant discrepancies or errors. In contrast, theory, although having certain limitations, can be applied to all of the above species and allows the derivation of a consistent set of molecular properties.

Unlike boron halides, whose adducts have received much theoretical attention,[3,8,14−16] there are only a few computational studies dealing with donor−acceptor compounds of Al, Ga, and In. A comparative investigation of donor−acceptor compounds MH_3-YH_3 of the B, Al, Ga, and In hydrides with ammonia and phosphine was presented in 1993 by Jungwirth and Zahradnik,[17] who applied the effective core potential LANL1DZ basis set at the self-consistent field (SCF) level of theory for gallium and indium. The structures of all adducts were found to be of C_{3v} symmetry with "staggered" orientation of the fragments. Dissociation energies obtained are in agreement with Pearson's hard and soft acid and base (HSAB) principle. Complexes of MH_3 with ammonia have been found to be stable under normal conditions, whereas the analogous complexes with phosphine are unstable.[17]

Jasien found in 1992 that donor molecules which bind via oxygen to the metal center form more stable adducts than donors which bind via chlorine.[18] A study[9] of complexes of HF and HCl with aluminum hydrides, fluorides, and chlorides demonstrated that the dissociation energies of HCl Lewis adducts are always much lower than those for the HF adducts with the same Lewis acid. The dissociation energies of adducts decreases in the order $AlF_3 > AlCl_3 > AlH_3$. The same trend was found for the complexes of AlX_3 and GaX_3 (X = H, F, Cl) with H_2O[19,20] and for AlX_3-OH^- (X = F, Cl) complexes.[21]

Bock et al. investigated the stability of adducts of substituted gallanes and arsines.[10] They obtained dissociation energies for several adducts, including GaF_3-AsH_3 and $GaCl_3-AsH_3$, and found that gallium fluoride is a stronger acceptor than gallium chloride. More recently, Jonas et al. presented a comparative study of Lewis acid−base complexes of BH_3, BF_3, BCl_3, $AlCl_3$, and SO_2 at the MP2 level of theory with a triple-ζ plus double-polarization basis set.[3] They found that strong boron complexes have a significant covalent contribution, while the strongly bonded aluminum complex $AlCl_3-NMe_3$ is mainly formed by electrostatic interactions. In agreement with experimental data, BCl_3 has been found to be a better acceptor than BF_3.

Branchadell et al. carried out a density functional study of complexes between boron and aluminum halides and ammonia and formaldehyde.[11] Using a triple-ζ basis set with polarization functions and the frozen core approximation for all the non-hydrogen atoms, they found that BCl_3 is a stronger acceptor than BF_3, in agreement with Jonas et al.[3] The situation is reversed for aluminum halides, and AlF_3 forms more stable complexes than $AlCl_3$ with both NH_3 and H_2CO.

Except for the recent work by Frenking et al.,[22] which is in part devoted to the donor−acceptor complexes of group 13 halides with H^- and water, only adducts of Al and Ga hydrides, fluorides, and chlorides were the subject of the ab initio studies. We investigate in the present work the influence of the donor molecule and the terminal halogen atoms of the metal halide acceptor on the donor−acceptor bond strength. The stability of weakly bonded adducts, formed by bromides and iodides, is of special interest, since their energies of formation apparently cannot be measured experimentally at this time. To include the bromine and iodine systems in this investigation, we used an effective core potential (ECP) basis set.

It was shown that the ECP method gives good results for gallium halides. In fact, Dai and Balasubramanian investigated ground and excited states of gallium halides (Cl, Br, I) using the CASSCF method with relativistic effective core potential basis sets.[23] Their results for $GaCl_3$ are in good agreement with other ab initio calculations. Furthermore, Duke et al.[24] investigated the chlorogallanes GaH_xCl_{1-x} ($x = 0-3$) and their dimers using both full electron and ECP basis sets. They concluded that polarization functions are necessary to reproduce the experimental geometry of the bridging region in Ga_2Cl_6. Compared to the SCF/DZP level of theory, the ECP method gives structures much closer to the equilibrium geometry than the all-electron method with the same basis set. According to the authors, this "remarkable agreement" with experiment is probably due to a cancellation of errors: while the ECP underestimates the bond lengths, inadequacies of the basis set increase the bond lengths.[24] A secondary goal of the present work was to test the applicability of the effective core potential method to the quantum chemical description of MX_3D_3 systems.

Computational Details

All calculations have been carried out using the GAUSSIAN 94 program package.[25] SCF and hybrid Hartree−Fock/density functional theory (B3LYP) using the exchange functional B3 by Becke[26] and the

(9) Wilson, M.; Coolidge, M. B.; Mains, G. J. *J. Phys. Chem.* **1992**, *96*, 4851.
(10) Bock, C. W.; Trachtman, M.; Mains, G. J. *J. Phys. Chem.* **1992**, *96*, 3007.
(11) Branchadell, V.; Sbai, A.; Oliva, A. *J. Phys. Chem.* **1995**, *99*, 6472.
(12) Timoshkin, A. Y. Ph.D. Thesis, St. Petersburg State University, 1997.
(13) Haaland, A. *Angew. Chem., Int. Ed. Engl.* **1989**, *28*, 992.
(14) Branchadell, V.; Oliva, A. *J. Mol. Struct.: THEOCHEM* **1991**, *236*, 75.
(15) Andres, J.; Arnau, A.; Bertran, J.; Silla, E. *J. Mol. Struct.: THEOCHEM* **1985**, *120*, 315.
(16) Branchadell, V.; Oliva, A. *J. Am. Chem. Soc.* **1991**, *113*, 4132.
(17) Jungwirth, P.; Zahradnik, R. *J. Mol. Struct.: THEOCHEM* **1993**, *283*, 317.
(18) Jasien, P. G. *J. Phys. Chem.* **1992**, *96*, 9273.
(19) Ball, D. W. *J. Phys. Chem.* **1995**, *99*, 12786.
(20) Grencewicz, K. A.; Ball, D. W. *J. Phys. Chem.* **1996**, *100*, 5672.
(21) Scholz, G.; Stosser, R.; Bartoll, J. *J. Phys. Chem.* **1996**, *100*, 6518.
(22) Frenking, G.; Fau, S.; Marchand, C. M.; Grützmacher, H. *J. Am. Chem. Soc.* **1997**, *119*, 6648.
(23) Dai, D.; Balasubramanian, K. *J. Chem. Phys.* **1993**, *99*, 293.
(24) Duke, B. J.; Hamilton, T. P.; Schaefer, H. F. *Inorg. Chem.* **1991**, *30*, 0, 4225.
(25) Frisch, M. J.; Trucks, G. W.; Schlegel, H. B.; Gill, P. M. W.; Johnson, B. G.; Robb, M. A.; Cheeseman, J. R.; Keith, T.; Petersson, G. A.; Montgomery, J. A.; Raghavachari, K.; Al-Laham, M. A.; Zakrzewski, V. G.; Ortiz, J. V.; Foresman, J. B.; Cioslowski, J.; Stefanov, B. B.; Nanayakkara, A.; Challacombe, M.; Peng, C. Y.; Ayala, P. Y.; Chen, W.; Wong, M. W.; Andres, J. L.; Replogle, E. S.; Gomperts, R.; Martin, R. L.; Fox, D. J.; Binkley, J. S.; Defrees, D. J.; Baker, J.; Stewart, J. P.; Head-Gordon, M.; Gonzalez, C.; Pople, J. A., Gaussian 94, Revision C.3.

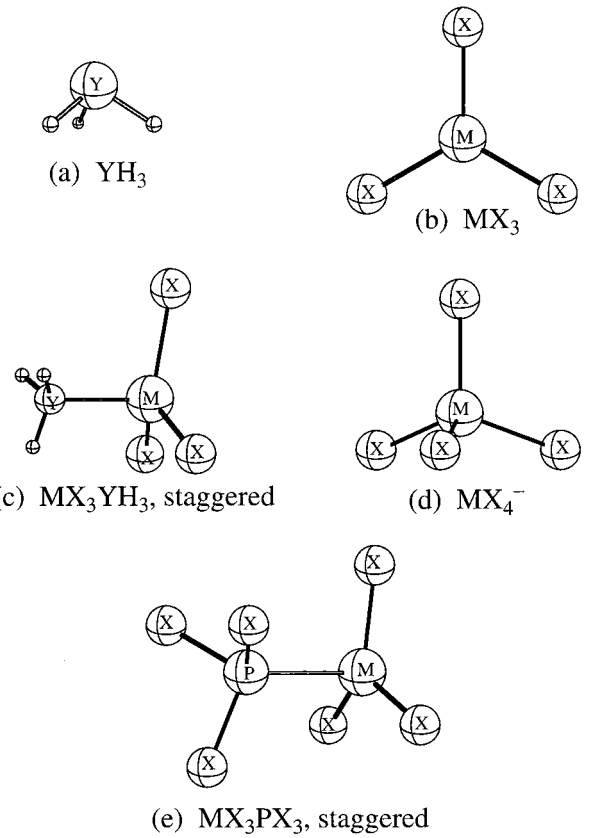

Figure 1. Geometries of the donor (a), acceptor (b), staggered conformation for the MX_3YH_3 complex (c), MX_4^- (d), and MPX_6 and ethane-like (e) compounds.

correlation functional LYP by Lee, Yang, and Parr[27] were applied in this work. For all systems under investigation, the standard LANL2DZP basis set was employed, which includes a valence double-ζ plus the ECP description,[28−30] augmented by one set of polarization functions. The following orbital exponents were used: p exponent for H (1.0) and d exponents for Al (0.4), Ga (0.16), In(0.16), N (0.8), P (0.4), As (0.25), F (0.8), Cl (0.56), Br (0.25), and I (0.15). Donors, acceptors, and MX_3YH_3 complexes were optimized under C_{3v}, D_{3h}, and C_{3v} restrictions, respectively (Figure 1). As shown by both experimental[31] and theoretical[17,32] studies, these geometries correspond to minima on the potential energy surface. T_d symmetric structures are the most stable for MX_4^- anions. Harmonic vibrational frequencies and infrared intensities were obtained by vibrational analysis of fully optimized geometries. The dissociation energies were corrected for zero point vibrational energies (ZPVE) obtained at the B3LYP/LANL2DZP level of theory from unscaled harmonic vibrational frequencies. Thermal corrections also have been made to enable comparison with the experimental data (298.15 K, 1 atm). Atomic charges were determined using Mulliken population analyses. The basis set superposition error (BSSE) correction was evaluated by the counterpoise method.[33]

Results and Discussion

I. Comparison of Experimental and Theoretical Data. A. Donor and Acceptor Molecules. The theoretical characteristics for the donor and acceptor molecules are presented in Tables 1 and 2, respectively. The donor geometries, the dipole moments, and the B3LYP vibrational frequencies are in good agreement with experiment.[34−38] The M−X distances are longer than determined experimentally, with an average difference of 3%. These discrepancies are about 0.05 Å, and may arise from the distortion of the planar MX_3 molecules in the high-temperature gas-phase electron diffraction experiment. Such experimental "bond shortening" is significant for metal iodides; e.g., for zinc iodide it is known to be about 0.05 Å.[39] The harmonic vibrational frequencies of MX_3 species also are in good agreement with experimental data.[38] Note that some of the experimental data are estimated[40−42] (e.g., A_1' for GaF_3), and in such cases the computed values are expected to be more reliable.

B. Adducts MX_3YH_3. Direct experimental gas-phase structural and thermodynamic data are known only for several ammonia adducts. Results for these species are presented in Tables 3 and 4, respectively.

In contrast to previous assessments,[43] the preliminary study with the nonpolarized LANL2DZ basis set suggests that polarization functions are essential for the correct description of structural and energetic characteristics of ammonia adducts. Whereas the nonpolarized basis set gives structural parameters similar to LANL2DZP, it fails for the dissociation energy: SCF/LANL2DZ overestimates this property of the donor−acceptor bond by 40−60 kJ mol^{-1}. The addition of one set of polarization functions significantly improves the agreement with the experimental data, which are obtained at high temperatures (600−800 K). Interestingly, the difference between SCF and B3LYP is no more that 6 kJ mol^{-1}, and B3LYP gives higher dissociation energies of the donor−acceptor bond than SCF. From Tables 3 and 4 we can conclude that both the SCF and B3LYP methods in combination with the LANL2DZP basis set give a good description of both structural and thermodynamic properties.

The calculated dissociation energies are on average 7 kJ mol^{-1} *higher* than experimental values (Table 4), except that for $GaBr_3$-NH_3 where the computed dissociation energy is *lower* than experiment. Our computed results for arsine adducts with GaF_3 and $GaCl_3$ are in good agreement with previous MP4(SDTQ) results of Bock et al.[10] The unusually large deviation from experiment for $GaBr_3NH_3$ suggests that the experiment might be in error. Since ΔH^{diss} and ΔS^{diss} values were derived experimentally in a tensimetric study (vapor pressure data),[6] and since $\log K^{diss} = -\Delta H^{diss}/RT + \Delta S^{diss}/R$, there is a strong correlation between ΔH^{diss} and ΔS^{diss}. Hence, an error in the ΔH^{diss} determination will lead to an error in the ΔS^{diss} determination. Indeed, the calculated and experimental values for the reaction entropy ΔS^{diss} for the $GaBr_3NH_3$ system differ in a manner similar to that of the dissociation enthalpy ΔH^{diss}. The

(26) Becke, A. D. *J. Chem. Phys.* **1993**, *98*, 5648.
(27) Lee, C.; Yang, W.; Parr, R. G. *Phys. Rev. B* **1988**, *37*, 785.
(28) Hay, P. J.; R., W. W. *J. Chem. Phys.* **1985**, *82*, 270.
(29) Hay, P. J.; R., W. W. *J. Chem. Phys.* **1985**, *82*, 299.
(30) Wadt, W. R.; Hay, P. J. *J. Chem. Phys.* **1985**, *82*, 284.
(31) Hargittai, M.; Hargittai, I. *The Molecular Geometries of Coordination Compounds in the Vapour Phase*; Elsevier: Amsterdam, 1977.
(32) Graves, R. M.; Scuseria, G. E. *J. Chem. Phys.* **1992**, *96*, 3723.
(33) Boys, S. F.; Bernardi, F. *Mol. Phys.* **1970**, *19*, 553.
(34) *Landolt-Börnstein*; Kuchitsu, K., Ed.; Springer-Verlag: Berlin, 1998; Vol. II/25a.
(35) *Landolt-Börnstein*; Hellwege, K.-H., Ed.; Springer-Verlag: Berlin, 1974; Vol. II/6.
(36) *Landolt-Börnstein*; Madelung, O., Ed.; Springer-Verlag: Berlin, 1992; Vol. II/19c.
(37) *Landolt-Börnstein*; Hellwege, K.-H., Ed.; Springer-Verlag: Berlin, 1982; Vol. II/14a.
(38) Nakamoto, K. *Infrared and Raman Spectra of Inorganic and Coordination Compounds*, 4th ed.; Wiley: New York, 1986.
(39) Domenicano, A.; Hargittai, I. *Accurate Molecular Structures*; Oxford University Press: London, 1992.
(40) Barin, I. *Thermochemical Data of Pure Substances*; VCH: Weinheim, 1989; Vols. I and II.
(41) Giricheva, N. I.; Lapshina, S. B.; Girichev, G. V. *Zh. Struct. Khim.* **1996**, *37*, 859.
(42) Hargittai, M. *Stereochemical Applications of Gas-Phase Electron Diffraction*; VCH: New York, 1987.
(43) Marsh, C. M. B.; Hamilton, T. P.; Xie, Y.; Schaefer, H. F. *J. Chem. Phys.* **1992**, *96*, 5310.

Table 1. Theoretical and Experimental Results for Donor Molecules YR_3[a]

						vibrational frequencies and infrared intensities[b]			
YR_3	method	R_{Y-R}	R−Y−R	μ	$S°_{(298)}$	A_1	E	A_1	E
NH_3	SCF/LANL2DZP	1.001	108.2	1.81	191.8	1114 (232)	1802 (25)	3728 (0.2)	3872 (3.4)
	B3LYP/LANL2DZP	1.018	107.1	1.85	192.3	1040 (191)	1679 (22)	3499 (0.3)	3636 (0.8)
	exptl	1.014	107.2	1.47	192.8	932/968	1628	3336/3338	3414
PH_3	SCF/LANL2DZP	1.407	95.5	0.86	209.4	1128 (33)	1258 (21)	2565 (22)	2571 (87)
	B3LYP/LANL2DZP	1.425	93.3	0.88	209.9	1046 (31)	1157 (13)	2395 (30)	2409 (70)
	exptl	1.413	93.5	0.57	210.3	990/992	1121	2327	2421
AsH_3	SCF/LANL2DZP	1.512	94.3	0.44	222.1	1017 (36)	1119 (18)	2320 (36)	2324 (111)
	B3LYP/LANL2DZP	1.528	92.2	0.39	222.6	949 (25)	1034 (10)	2180 (42)	2191 (85)
	exptl	1.513	92.1	0.22	222.8	906	1005	2122	2185
PF_3	SCF/LANL2DZP	1.561	97.2	1.39	270.9	523 (42)	373 (7)	972 (168)	929 (230)
	B3LYP/LANL2DZP	1.598	97.5	1.37	274.7	458 (26)	324 (5)	874 (129)	835 (188)
	exptl	1.561	97.7	1.13	273.0	487	346	893	858
PCl_3	SCF/LANL2DZP	2.047	100.3	1.00	307.7	286 (5)	208 (0.8)	559 (53)	555 (177)
	B3LYP/LANL2DZP	2.087	100.7	0.95	313.5	248 (2)	179 (0.3)	504 (41)	485 (161)
	exptl	2.039	100.3	0.56	311.7	258	186	515	504
PBr_3	SCF/LANL2DZP	2.249	101.3	0.44	345.3	173 (0.2)	122 (0)	407 (16)	421 (103)
	B3LYP/LANL2DZP	2.287	101.8	0.51	351.6	150 (0.04)	104 (0.03)	372 (11)	368 (105)
	exptl	2.220	101.0		348.2	160	113	390	384
PI_3	SCF/LANL2DZP	2.481	102.6	0.16	371.8	120 (0.003)	84 (0.05)	320 (4)	351 (61)
	B3LYP/LANL2DZP	2.518	103.1	0.01	378.4	105 (0.03)	72 (0.1)	296 (3)	304 (78)
	exptl				374.4	111	79	303	325

[a] All distances in Å, angles in deg, dipole moments in D, entropies in J K^{-1} mol^{-1}, vibrational frequencies in cm^{-1}, and infrared intensities (in parentheses) in km mol^{-1}. Experimental geometries are taken from ref 34, dipole moments from refs 35−37, experimental entropy values from ref 40, and vibrational frequencies from ref 38. [b] The intensities of degenerate modes have not been doubled.

Table 2. Theoretical and Experimental Results for Acceptor Molecules MX_3[a]

				vibrational frequencies and infrared intensities[c]			
MX_3	method	R_{M-X}	$S°_{(298)}$	E′	A_2''	A_1'	E′
AlF_3	SCF/LANL2DZP	1.614	275.0	267 (47)	321 (197)	725 (0)	1002 (236)
	B3LYP/LANL2DZP[d]	1.633	286.1	253 (37)	301 (150)	689 (0)	953 (181)
	exptl	1.630 ± 0.003	276.7	252	284	⟨660⟩[b]	960
GaF_3	SCF/LANL2DZP	1.653	285.9	233 (45)	239 (104)	699 (0)	778 (107)
	B3LYP/LANL2DZP	1.676	288.9	214 (34)	221 (72)	648 (0)	724 (81)
	exptl	1.716	292.9	190	200	⟨700⟩[b]	759
InF_3	SCF/LANL2DZP	1.787	298.9	184 (50)	189 (102)	622 (0)	645 (87)
	B3LYP/LANL2DZP	1.811	302.4	166 (39)	175 (70)	577 (0)	601 (68)
	exptl	⟨2.0⟩[b]	310.0	130	150	600	⟨640⟩[b]
$AlCl_3$	SCF/LANL2DZP	2.064	309.9	162 (12)	219 (63)	405 (0)	648 (221)
	B3LYP/LANL2DZP	2.079	312.5	151 (9)	204 (42)	381 (0)	619 (180)
	exptl	2.068 ± 0.004	314.5	151	214	375	616
$GaCl_3$	SCF/LANL2DZP	2.109	322.2	139 (12)	156 (25)	384 (0)	471 (98)
	B3LYP/LANL2DZP	2.128	325.8	127 (9)	142 (16)	357 (0)	446 (82)
	exptl	2.100 ± 0.002	325.1	128	145	382	450
$InCl_3$	SCF/LANL2DZP	2.276	335.5	111 (15)	116 (28)	353 (0)	400 (72)
	B3LYP/LANL2DZP	2.298	339.3	101 (11)	105 (19)	329 (0)	377 (60)
	exptl	2.289	341.4	95	110	350	394
$AlBr_3$	SCF/LANL2DZP	2.250	346.0	97 (3)	183 (26)	239 (0)	516 (180)
	B3LYP/LANL2DZP	2.264	349.0	90 (2)	169 (17)	226 (0)	494 (149)
	exptl	2.223 ± 0.005	349.4	93	107	228	450−500
$GaBr_3$	SCF/LANL2DZP	2.287	357.7	88 (3)	124 (10)	230 (0)	352 (77)
	B3LYP/LANL2DZP	2.304	361.5	81 (2)	113 (6)	214 (0)	333 (65)
	exptl	2.246 ± 0.003	363.7	84	95	219, 237	
$InBr_3$	SCF/LANL2DZP	2.448	370.5	72 (5)	89 (11)	215 (0)	286 (54)
	B3LYP/LANL2DZP	2.469	374.5	66 (3)	81 (7)	200 (0)	270 (45)
	exptl	⟨2.30⟩[b]	373.4	62	74	212	280
AlI_3	SCF/LANL2DZP	2.469	371.0	70 (1)	157 (10)	166 (0)	438 (156)
	B3LYP/LANL2DZP	2.479	374.2	64 (0.7)	144 (6)	156 (0)	419 (132)
	exptl		373.6	64	77	156	370−410
GaI_3	SCF/LANL2DZP	2.499	383.0	63 (1)	105 (4)	161 (0)	291 (68)
	B3LYP/LANL2DZP	2.513	386.6	58 (0.8)	96 (2)	149 (0)	275 (58)
	exptl	2.458 ± 0.005	390.1	50	63	147	275
InI_3	SCF/LANL2DZP	2.657	395.5	52 (2)	74 (5)	151 (0)	231 (47)
	B3LYP/LANL2DZP	2.675	399.6	47 (1)	67 (3)	140 (0)	219 (40)
	exptl	2.617	400.0	44	56	151	200−230

[a] All distances in Å, entropies in J K^{-1} mol^{-1}, vibrational frequencies in cm^{-1}, and infrared intensities (in parentheses) in km mol^{-1}. Experimental entropy values are taken from ref 40, experimental geometries from refs 41 and 42, and vibrational frequencies from refs 38 and 41. [b] Data are estimated. [c] The intensities of degenerate modes have not been doubled. [d] The D_{3h} geometry optimization did not converge; the data given are mean values of a C_{2v} structure which is almost D_{3h} symmetric. The E′ modes are the mean values of its A_1 and B_2 components.

Table 3. Theoretical and Experimental Geometrical Parameters for MX_3NH_3 Adducts[a]

MX_3NH_3	method	R_{M-N}	R_{M-X}	R_{N-H}	X−M−Y	X−M−X	H−N−H
$AlCl_3NH_3$	SCF/LANL2DZ	2.015	2.198	1.009	100.8		
	SCF/LANL2DZP	2.012	2.120	1.006	101.1	116.4	107.7
	B3LYP/LANL2DZP	2.021	2.123	1.023	100.8	116.6	107.6
	exptl	1.998 ± 0.019	2.102 ± 0.005	(1.030)[b]		116.9 ± 0.4	112.8 ± 3.5
$AlBr_3NH_3$	SCF/LANL2DZ	2.028	2.373	1.009	101.0		
	SCF/LANL2DZP	2.010	2.301	1.007	101.2	116.3	107.9
	B3LYP/LANL2DZP	2.022	2.312	1.023	100.8	116.6	107.9
	exptl	1.999 ± 0.019	2.266 ± 0.005	1.063 ± 0.033		116.1 ± 0.3	114.5 ± 4.0
$GaCl_3NH_3$	SCF/LANL2DZ	2.031	2.201	1.008	100.8		
	SCF/LANL2DZP	2.055	2.156	1.006	100.7	116.6	108.3
	B3LYP/LANL2DZP	2.065	2.173	1.022	100.3	116.9	108.3
	exptl	2.058 ± 0.011	2.144 ± 0.005	1.030 ± 0.012		117.1 ± 0.3	114.3 ± 1.2
$GaBr_3NH_3$	SCF/LANL2DZ	2.045	2.372	1.008	100.9		
	SCF/LANL2DZP	2.060	2.338	1.006	100.5	116.7	108.3
	B3LYP/LANL2DZP	2.072	2.353	1.022	100.1	117.0	108.4
	exptl	2.082 ± 0.023	2.290 ± 0.005	1.063 ± 0.033		116.6 ± 0.3	115.6 ± 4.1

[a] All distances in Å, angles in deg. Experimental data are taken from ref 42. [b] Estimated value.

Table 4. Theorectial $\Delta H^{diss}_{(298)}$, $\Delta S^{diss}_{(298)}$, and $\Delta G^{diss}_{(298)}$ and Experimental Gas-Phase Dissociation Enthalpies, Gibbs Energies (kJ mol^{-1}), and Entropies (J mol^{-1} K^{-1}) for Adducts MX_3NH_3[a]

MX_3NH_3	method	$\Delta H^{diss}_{(298)}$	$\Delta S^{diss}_{(298)}$	$\Delta G^{diss}_{(298)}$	q_{CT}
$AlCl_3NH_3$	SCF/LANL2DZ	195.4	141.4	153.2	0.191
	SCF/LANL2DZP	154.6	137.3	113.7	0.220
	B3LYP/LANL2DZP	156.7	136.1	116.1	0.244
	exptl	137.1 ± 5.9	120.4 ± 6.3	101.2 ± 7.8	
$AlBr_3NH_3$	SCF/LANL2DZ	177.9	142.3	135.5	0.198
	SCF/LANL2DZP	145.7	138.4	104.4	0.234
	B3LYP/LANL2DZP	148.3	135.2	108.0	0.253
	exptl	143.8 ± 4.6	140.9 ± 6.3	101.8 ± 6.5	
$GaCl_3NH_3$	SCF/LANL2DZ	182.7	140.6	140.8	0.235
	SCF/LANL2DZP	131.5	129.1	93.0	0.291
	B3LYP/LANL2DZP	137.8	147.7	93.8	0.326
	exptl	134.2 ± 2.5	141.3 ± 3.8	92.1 ± 3.6	
$GaBr_3NH_3$	SCF/LANL2DZ	162.5	141.8	99.5	0.239
	SCF/LANL2DZP	120.5	133.3	80.8	0.295
	B3LYP/LANL2DZP	125.4	123.7	88.5	0.328
	exptl	137.1 ± 0.8	157.6 ± 2.5	90.1 ± 1.5	
$InCl_3NH_3$	SCF/LANL2DZ	170.7	125.6	133.3	0.188
	SCF/LANL2DZP	132.5	142.9	89.9	0.196
	B3LYP/LANL2DZP	134.3	141.3	92.2	0.235
	exptl	112.1 ± 5.4	117.5 ± 7.1	77.1 ± 7.5	
$InBr_3NH_3$	SCF/LANL2DZ	154.2	128.8	115.8	0.195
	SCF/LANL2DZP	120.3	143.5	77.5	0.199
	B3LYP/LANL2DZP	123.8	142.2	81.4	0.237
	exptl	114.1 ± 6.3	129.6 ± 8.4	75.5 ± 8.8	

[a] Theoretical standard enthalpies are given with ZPVE but without BSSE corrections; experimental data are measured in the temperature range 600−800 K.

Table 5. Theoretical ($T = \Delta H^{diss}_{(298)}/\Delta S^{diss}_{(298)}$) and Experimental Values of Temperature (K) for Which $K^{diss} = 1$

method	$AlCl_3NH_3$	$AlBr_3NH_3$	$GaCl_3NH_3$	$GaBr_3NH_3$	$InCl_3NH_3$	$InBr_3NH_3$
SCF/LANL2DZ	1382	1250	1299	1146	1359	1197
SCF/LANL2DZP	1126	1053	1019	904	927	838
B3LYP/LANL2DZP	1151	1097	933	1014	950	871
exptl	1139	1021	950	870	954	880

experimentally derivedentropy of reaction ΔS^{diss} is higher than the theoretical value and also significantly higher than ΔS^{diss} for other adducts.

A similar discrepancy between experiment and theory is found for the $GaBr_3NH_3$ system when the temperature $T = \Delta H^{diss}_{(298)}/\Delta S^{diss}_{(298)}$ (Table 5) is considered, at which the equilibrium constant K^{diss} for the following process equals 1:

$$MX_3YH_3(g) \rightleftharpoons MX_3(g) + YH_3(g)$$

Only for the $GaBr_3NH_3$ system the difference between theory and experiment is more than 100 K, whereas there is remarkably good (within 20 K) agreement between the B3LYP and experimental values for all other MX_3YH_3 complexes. This discrepancy between experiment and theory suggests that there exists another process under the experimental gas-phase conditions, which increases the entropy, in addition to the $GaBr_3NH_3 \rightleftharpoons GaBr_3 + NH_3$ equilibrium. It was shown for $AlCl_3NH_3$ that thermal destruction to AlN goes through a series of oligomer forms.[44] Similarly, formation of HBr and $^1/_2(Br_2GaNH_2)_2$ may accompany the dissociation process within the temperature range studied experimentally, leading to higher values of entropy and enthalpy.

(44) Timoshkin, A. Y.; Bettinger, H. F.; Schaefer, H. F. *J. Am. Chem. Soc.* **1997**, *119*, 5668.

Jonas et al.[3] found that the theoretically predicted dissociation energies at the SCF level are too low for boron complexes, and that the corresponding interatomic distances are too long. In contrast, the dissociation energies computed at the SCF/LANL2DZP level are higher than experimental values, while the calculated M−N distances are in excellent agreement with experiment (Table 3).

A full set of structural and thermodynamic properties of all 36 distinct complexes is available in the Supporting Information. Later in this paper we will discuss several aspects of MX_3-YH_3 adduct formation in detail.

II. MX_3-YH_3 Systems (M = Al, Ga, In; X = F, Cl, Br, I; Y = N, P, As). A. Eclipsed and Staggered Orientations. According to previous theoretical studies, $R_3M-YR'_3$ adducts have C_{3v} symmetry with a staggered orientation of the fragments.[17,32] This conformation is also assumed in interpreting experimental gas-phase electron diffraction data.[31,42] We find that, for some adducts of MF_3, the staggered conformer is a transition state for the rotation around the donor−acceptor bond. The eclipsed InF_3NH_3 conformation was found to be a minimum at both SCF and B3LYP levels of theory. The rotational barrier is only 2.3 kJ mol^{-1} at 0 K (including ZPVE), and it becomes nearly zero at room temperature, when thermal corrections for each conformer are taken into account. The low rotational barrier indicates that the structures of the adducts are very flexible, and the rate of conformational exchange should be high. Low rotational barriers were also obtained for the staggered $AlCl_3$-NH_3 (0.6 kJ mol^{-1} at the B3LYP/DZP level of theory)[44] and for ammonia alane (3.1 kJ mol $^{-1}$ at the CCSD/DZP level of theory).[43] The stabilization of eclipsed structures with short H−X distances may result from electrostatic (Coulomb) interactions between the terminal H and X atoms. The existence of such intramolecular interactions was found experimentally in the solid $Cy_2BrGaNH_2Ph$ (Cy = cyclohexyl) adduct,[45] and they were also predicted by theory for $AlCl_3$−ClHCO.[46] Experimental rotational barriers for some solid complexes of BF_3 with NH_3, pyridine, and CH_3CN are in the 8−18 kJ mol^{-1} range.[47] Larger experimental values may arise from additional intermolecular interactions in the solid state.

B. Basis Set Superposition Error. The basis set of each fragment is extended by the basis functions of the other fragment under adduct formation. This effect is called basis set superposition error[48,49] and may be considered using the counterpoise function by Boys and Bernardi.[33] It was shown for He_2[50] that the Boys−Bernardi scheme agrees within 0.001 K with an estimated infinite basis set. However, the counterpoise method overestimates the value of BSSE for strongly bound complexes. It was found as early as 1986 that calculated BSSE values for some H-bonded complexes provide unreasonable agreement with experimental data.[51]

For hydride complexes MH_3-YH_3 (M = Al, Ga, In; Y = N, P, As) the superposition error depends on the basis set employed.[17] In fact the correction is about 40−80 kJ mol^{-1} with a minimal basis set at the SCF level and 12−24 kJ mol^{-1} with a split-valence basis without polarization functions. With a DZP quality basis set, the BSSE correction for $AlCl_3$−ClHCO is 4 kJ mol^{-1} at SCF and 17 kJ mol^{-1} at the MP2 level of theory.[46] BSSE ranges from 2 to 24 kJ mol^{-1} for the eight complexes of boron and aluminum halides with HCl and HF,[52] and is about 10 kJ mol^{-1} for $Al(F,Cl)_3-H_2O$ complexes at MP2/6-31G-(d,p).[19] Jasien argued that the core electrons do not contribute to BSSE when ECP is used, as they are replaced by the effective potential.[18] Thus, BSSE may not be significant for the donor−acceptor interaction computed.[5,18] On the other hand, it was shown by Jungwirth and Zahradnik that for the aluminum hydride adduct with ammonia the correction to the dissociation energy ranges from 40 to 80 kJ mol^{-1} with an ECP minimal basis set.[17]

Table 6. Distortion Energy E^{dist} and BSSE Value E^{BSSE} for Donor and Acceptor Fragments of Some Adducts (kJ mol^{-1})

	donor (YH_3) fragment				acceptor (MX_3) fragment			
	SCF		B3LYP		SCF		B3LYP	
complex	E_D^{dist}	E_D^{BSSE}	E_D^{dist}	E_D^{BSSE}	E_A^{dist}	E_A^{BSSE}	E_A^{dist}	E_A^{BSSE}
AlF_3NH_3	0.1	−5.0	0.2	−8.0	32.7	−5.2	27.6	−8.0
$AlCl_3NH_3$	0.2	−4.7	0.2	−7.6	34.8	−5.8	28.5	−6.3
$AlCl_3PH_3$	9.1	−2.2	9.5	−2.7	30.9	−5.5	22.7	−6.1
$AlCl_3AsH_3$	9.5	−1.8	9.3	−1.6	29.5	−5.9	21.8	−6.7
InI_3AsH_3	7.8	−1.8	7.0	−1.7	15.8	−1.2	10.2	−1.5

Table 7. Total BSSE Correction E^{BSSE} and Total Correction $E^{BSSE} + E^{dist}$ for Some Adducts (kJ mol^{-1})

	SCF			B3LYP		
complex	E^{BSSE}	$E^{BSSE} + E^{dist}$	$\Delta H^{diss}_{(298)}$	E^{BSSE}	$E^{BSSE} + E^{dist}$	$\Delta H^{diss}_{(298)}$
AlF_3NH_3	−10.2	22.6	165.6	−16.0	11.8	135.1
$AlCl_3NH_3$	−10.5	24.5	154.6	−13.9	14.8	156.7
$AlCl_3PH_3$	−7.7	32.3	67.0	−8.8	23.4	64.6
$AlCl_3AsH_3$	−7.7	31.3	53.4	−8.3	22.8	49.9
InI_3AsH_3	−3.0	20.2	34.5	−3.2	14.0	29.6

Under adduct formation acceptor and donor fragments are distorted, and the calculated energy will include both the sum of the distortion energies of the fragments and BSSE. To separate those two factors, we used the following scheme, where the same geometries are used as in the optimized adduct structure for A and D. The energy of each fragment is calculated with and without ghost orbitals of the other fragment. The energy difference between free and distorted A gives as a distortion energy E_A^{dist} for the acceptor. The energy difference between free and distorted A with ghost orbitals of the other fragment gives the sum of E_A^{BSSE} and E_A^{dist}. The same procedure was applied to the donor fragment D, resulting in E_D^{BSSE} and E_D^{dist}. The sum of E_A^{BSSE} and E_D^{BSSE} gives the total BSSE correction to the energy of formation for the corresponding adduct E_{AD}^{BSSE}. The sum $E_A^{dist} + E_D^{dist}$ characterizes the total distortion energy E_{AD}^{dist} for the adduct. Theoretical data for several complexes are presented in Table 6.

Whereas the distortion energy for NH_3 is small (0.2 kJ mol^{-1}), E_D^{dist} increases up to 7−9 kJ mol^{-1} for phosphine and arsine, depending on the acceptor strength of the partner. On the other hand, BSSE is most pronounced for NH_3 (−8 kJ mol^{-1}) and decreases toward PH_3 (−3 kJ mol^{-1}) and AsH_3 (−2 kJ mol^{-1}). This is due to the donor−acceptor (DA) bond strength decreasing and to the diffuseness of the lone pairs in PH_3 and AsH_3. The pyramidalization of the acceptor molecules leads to a E_A^{dist} which is significantly larger than E_D^{dist} for donors. The maximal value of E_A^{dist} is 35 kJ mol^{-1}, in good agreement with early

(45) Atwood, D. A.; Cowley, A. H. *J. Organomet. Chem.* **1992**, *430*, C29.
(46) Jasien, P. G. *J. Phys. Chem.* **1994**, *98*, 2859.
(47) Prout, C. K.; Kamenar, B. *Molecular Complexes*; Elek Science: London, 1973; Vol. 1.
(48) Hobza, P.; Zahradnik, R. *Intermolecular Complexes*; Academia: Prague, 1988.
(49) Clark, T. *A Handbook of Computational Chemistry*; Wiley: New York, 1985.
(50) Gutowski, M.; van Duijneveldt-van de Rijdt, J. G. C. H.; van Lenthe, J. H.; van Duijneveldt, F. B. *J. Chem. Phys.* **1993**, *98*, 4728.
(51) Frisch, M. J.; Del Bene, J. L.; Binkley, J. S.; Schaefer, H. F. *J. Chem. Phys.* **1986**, *84*, 2279.
(52) Scholz, G. *J. Mol. Struct.: THEOCHEM* **1994**, *309*, 227.

Table 8. Distortion Energies and BSSE Correction for $AlCl_3NH_3$ (kJ mol^{-1}) Evaluated with Different Methods and Basis Sets

	NH_3		$AlCl_3$		total for $AlCl_3NH_3$			
method/basis set	E^{BSSE}	E^{dist}	E^{BSSE}	E^{dist}	E^{BSSE}	E^{dist}	$E^{BSSE} + E^{dist}$	$\Delta H^{diss}_{(298)}$
SCF/DZP	−6.2	0.2	−2.7	34.1	−8.9	34.3	25.4	149.1
SCF/LANL2DZP	−4.7	0.2	−5.8	34.8	−10.5	35.0	24.5	154.6
B3LYP/DZP	−9.7	0.2	−4.9	28.2	−14.6	28.4	13.8	149.0
B3LYP/LANL2DZP	−7.7	0.2	−6.3	28.5	−14.0	28.7	14.7	156.7

predictions[10] of about 30 kJ mol^{-1}. The total BSSE corrections (Table 7) lie in the −3 to −14 kJ mol^{-1} (B3LYP) and −3 to −10 kJ mol^{-1} (SCF) ranges, and decrease with decreasing donor−acceptor bond dissociation energy.

It was shown by Matsuzawa and Osamura for the benzene−Cl_2 complex that the frozen core approximation at the MP2 level of theory leads to an inadequate BSSE description.[53] To investigate the influence of the ECP basis sets on BSSE, the $AlCl_3NH_3$ adduct was studied at the SCF/DZP and B3LYP/DZP levels of theory. The results obtained differ by no more than 2 kJ mol^{-1} between LANL2DZP and DZP basis sets (Table 8).

Finally, we conclude that BSSE is significant for small basis sets without polarization functions. For basis sets of DZP quality, BSSE is about 2−24 kJ mol^{-1}, and for the LANL2DZP basis set it ranges from 3 to 14 kJ mol^{-1}. BSSE decreases in the order NH_3 > PH_3 > AsH_3 in accordance with the decreasing complex dissociation energy. At the SCF level of theory, the total correction to the donor−acceptor bond dissociation energy is 6−10 kJ mol^{-1} higher than at the B3LYP level.

C. Electron Correlation Effects. In this section we discuss the influence of electron correlation on the donor−acceptor complexes. As was shown by Jasien,[18] the inclusion of electron correlation has a relatively small influence on the calculated dissociation energies of complexes between aluminum chloride and strong O-bonded donors: the dissociation energy increases by 3.8 and 9.6 kJ mol^{-1} for H_2CO and HClCO, respectively, at the MP2 level of theory compared to SCF with the same basis set. For $AlCl_3EtCClO$, electron correlation increases the dissociation energy by 15.5 kJ mol^{-1} at the MP2/TZ2P basis set.[3] Marsh and Schaefer have shown that electron correlation adds 11.3 kJ mol^{-1} to the dissociation energy of ammonia alane, with no difference among the CISD, CISD+Q, and CCSD methods.[54]

The correlation effects were computed to be 11.7 kJ mol^{-1} for the arsine−trimethylgallium adduct at the CCSD level.[32] However, addition of methyl groups to the donor molecule increases the influence of the electron correlation dramatically: for trimethylamine alane [AlH_3−$N(CH_3)_3$] correlation adds 20.1, 25.1, and 26.2 kJ mol^{-1} to the dissociation energy, at the CISD, CISD(Q), and CCSD levels of theory with a DZP basis set.[54] According to MP2/TZ2P data, correlation adds 33.5 kJ mol^{-1} for NH_3−BCl_3 while for BCl_3−NMe_3 it adds 84 kJ mol^{-1} to the dissociation energy.[3] Similar results were obtained for the BF_3 adducts with ammonia (9.2 kJ mol^{-1}) and with trimethylamine (34.7 kJ mol^{-1}). Hence, electron correlation effects are more important for boron chlorides than for boron fluorides, and extremely important for methyl-substituted donor molecules.

In going from BCl_3−NMe_3 to $AlCl_3$−NMe_3, the contribution of electron correlation to the dissociation energy greatly decreases (by 34 kJ mol^{-1}).[3] The correlation effects are even less important in adducts between gallium halides and YH_3 donors; for GaF_3−AsH_3 and $GaCl_3$−AsH_3 correlation adds only 8.8 and 8.4 kJ mol^{-1}, respectively, at the MP4(SDTQ) level of theory.[10] We emphasize that correlation effects range between 0.9 and 12 kJ mol^{-1} for different types of adducts with simple YH_3 donors, and we ascribe an uncertainty of 15 kJ mol^{-1} to the influence of the correlation effects for the MX_3YH_3 complexes.

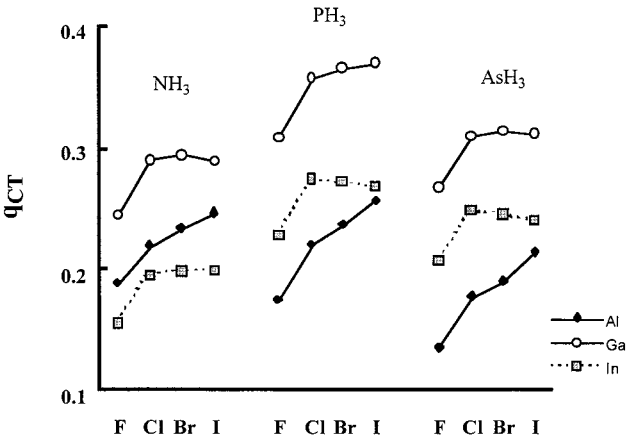

Figure 2. Total charge transfer for MX_3YH_3 complexes.

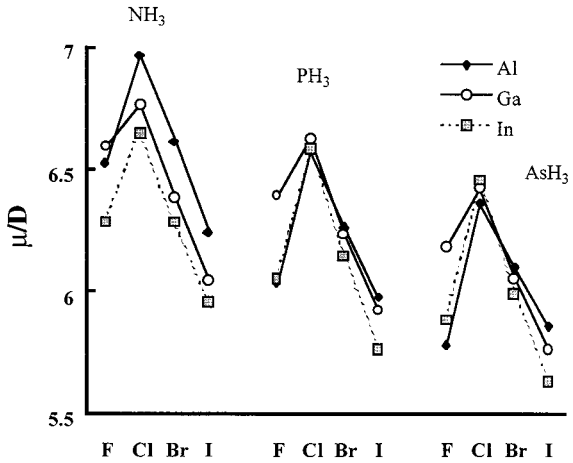

Figure 3. Dipole moments for MX_3YH_3 complexes.

Our ECP data (LANL2DZP) show (Table 4) that B3LYP increases the donor−acceptor dissociation energies by only 2−6 kJ mol^{-1} compared to SCF, in good agreement with previous computational studies using DZP quality basis sets. Note that BSSE and electron correlation effects approximately cancel each other. The absolute BSSE correction (3−14 kJ mol^{-1}) and B3LYP correlation contributions (2−6 kJ mol^{-1}) are close, and have opposite signs for ammonia adducts. The SCF level of theory (without BSSE correction) gives a remarkably good description of the structure and the thermodynamics of simple MX_3−NH_3 adducts, probably due to a cancellation of errors.[24]

D. Charge Transfer and Dissociation Energy. Charge transfer (q_{CT}), dipole moments, M−Y distances, and dissociation energies for MX_3YH_3 adducts are presented in the Figures 2−5, respectively. The theoretical dissociation energies (Figure 5) decrease from fluorides to iodides, in agreement with previous computational studies.[3,9−11] In contrast, the degree of charge

(53) Matsuzawa, H.; Osamura, Y. *Bull. Chem. Soc. Jpn.* **1997**, *70*, 1531.
(54) Marsh, C. M. B.; Schaefer, H. F. *J. Phys. Chem.* **1995**, *99*, 195.

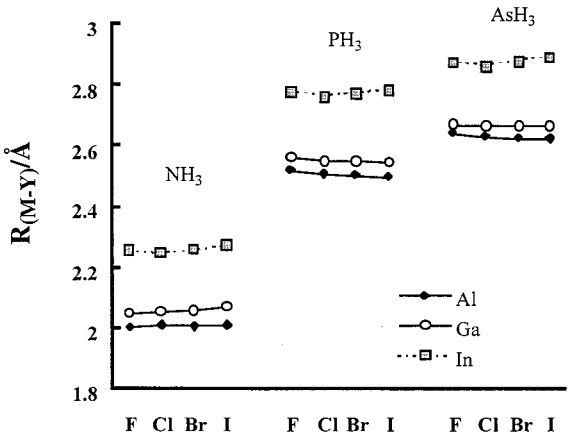

Figure 4. Donor−acceptor bond length, R_{M-Y} in MX_3YH_3 complexes. SCF/LANL2DZP level of theory.

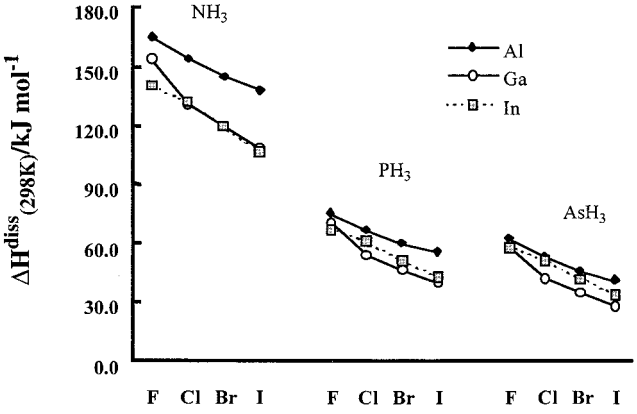

Figure 5. Theoretical dissociation enthalpies, $\Delta H^{diss}_{(298)}$ (kJ mol^{-1}) for MX_3YH_3 complexes.

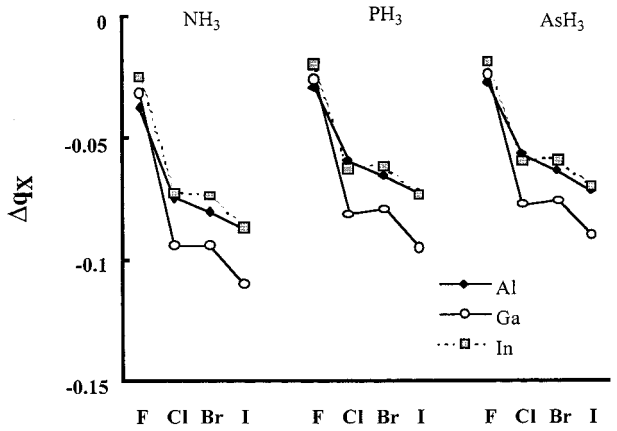

Figure 6. Change of the effective charge on the X atom: $\Delta q_X = q_X(MX_3YH_3) - q_X(MX_3)$. SCF/LANL2DZP level of theory.

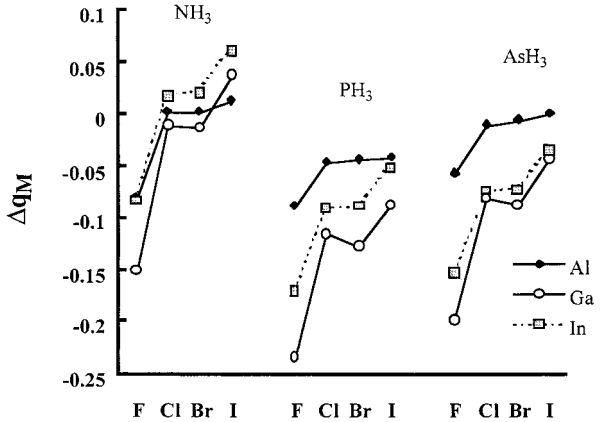

Figure 7. Change of the effective charge on the M atom: $\Delta q_M = q_M(MX_3YH_3) - q_M(MX_3)$. SCF/LANL2DZP level of theory.

transfer and the dipole moment (Figures 2 and 3) change nonmonotonically along the series MF_3, MCl_3, MBr_3, and MI_3: the MF_3 complexes behave exceptional. In fact, the calculated q_{CT} for the fluorine-containing adducts is 0.05*e* lower than that for chlorides. This is in contradiction to the generally accepted correlation between the charge-transfer q_{CT} and dissociation energy, $\Delta H^{diss} = Aq_{CT} + B$, which suggests that the adducts with the largest amount of charge transfer should have the highest dissociation energies.[2] However, such a correlation is not valid for MX_3YH_3 adducts. In the most stable fluorine complexes the amount of charge transfer is small; the complexes of PH_3 and AsH_3 have large q_{CT} values but are weakly bound.

Bock et al.[10] ascribed the different MX_3-YH_3 dissociation energies of fluorides and chlorides to the distortion energy, which is 29.7 kJ mol^{-1} for $GaCl_3$ and 26.3 kJ mol^{-1} for GaF_3. According to our data, the distortion energies of the fluorides are indeed 2−3 kJ mol^{-1} lower than for the chlorides (Table 6). But since the dissociation energy difference of GaF_3-NH_3 and $GaCl_3-NH_3$ adducts is 15−20 kJ mol^{-1} (Figure 5), it is clear that this large difference cannot be explained solely by the distortion energy.

The experimentally obtained linear $\Delta H^{diss}-q_{CT}$ relationship, which is in contrast to theory for MX_3YH_3 adducts, might arise from the experimental derivation of q_{CT}. The dipole moment of the MX_3YH_3 complex, $\mu_{complex}$, can be determined experimentally, but the dipole moment of the donor−acceptor bond μ_{DA} is calculated assuming that the dipole moment of the donor part is equal to the dipole moment of the free donor.[2] The dipole moment of the acceptor part is usually estimated similarly.[2] The charge transfer is obtained as $q_{CT} = \mu_{DA}/eR_{DA}$, where R_{DA} is the DA bond length, and *e* is the electron charge. However, this method completely ignores the charge redistribution accompanying complex formation. The dipole moments of the M−X and Y−H bonds in the complex will differ from their values in the free donor and acceptor molecules. Hence, the linear correlation of $\Delta H^{diss}-q_{CT}$ arises from a model which allows charge transfer only between donor and acceptor centers and ignores the effects of charge redistribution. Let us now consider the charge redistribution in these systems.

E. Charge Redistribution in Adducts. Charge is transferred from the donor to the acceptor during the formation of complexes between MX_3 and YH_3. To characterize the location of the transferred charge, we will use the change in effective atomic charges, as obtained by the Mulliken population analyses. Although the absolute values of atomic charges are arbitrary, the effective change in atomic charge should be more reliable. This redistribution of the Mulliken effective charges is presented in Figures 6 and 7.

We find that the fluorine systems differ from the other halides as the effective charge of the fluorine atoms is hardly affected by complex formation, and the total transferred charge is localized mostly on the metal atom. The situation is reversed for the other halides, where the X atoms accept up to 3/4 of the total charge transferred. The terminal H atoms of the donor moieties lose 0.1*e* each, regardless of charge transfer, while the central N, P, or As atoms contribute only 0.08*e*. Hence, the total charge transfer mostly stems from charge redistribution between terminal atoms: 3/4 of the charge is transferred from

Table 9. Electrostatic E_E and Covalent E_C Contributions to the Formation Enthalpy $\Delta H^{form}_{(298)}$ (kJ mol^{-1}) for Some Aluminum Halide Complexes at the SCF/LANL2DZP Level of Theory

	point charge contributions						
complex	E_{MY}	$3E_{MH}$	$3E_{YX}$	$6E_{HX}+3E'_{HX}$	E_E	E_C	$\Delta H^{form}_{(298)}$
AlF_3NH_3	−914	893	725	−789	−85	−81	−166
$AlCl_3NH_3$	−595	601	451	−520	−63	−92	−155
$AlBr_3NH_3$	−612	629	445	−482	−20	−126	−146
AlI_3NH_3	−565	587	399	−482	−61	−78	−139
AlF_3PH_3	73	66	−63	−63	13	−89	−76
$AlCl_3PH_3$	61	51	−52	−49	11	−78	−67
$AlBr_3PH_3$	71	54	−59	−51	15	−75	−60
AlI_3PH_3	71	55	−57	−52	17	−73	−56
AlF_3AsH_3	−102	164	88	−155	−5	−58	−63
$AlCl_3AsH_3$	−51	113	43	−107	−2	−51	−53
$AlBr_3AsH_3$	−47	119	38	−111	−1	−46	−47
AlI_3AsH_3	−34	111	27	−103	1	−43	−42

H to X atoms. As this significantly changes the dipole moments of terminal bonds in complexes as compared to free MX_3 and YH_3 molecules, the often used additivity scheme[2] is not valid for these complexes. We conclude that *there is no simple correlation* between dissociation energy and charge transfer.

F. Electrostatic Model. The significant charge redistribution in MX_3YH_3 systems suggests that the Coulomb interaction can be important for the stability of a MX_3YH_3 complex. According to the Mulliken population analyses, M atoms have positive and X atoms have negative charges. For instance, the electrostatic interactions $M^{\delta+}-Y^{\delta-}$ and $X^{\delta-}-H^{\delta+}$ will stabilize whereas the $M^{\delta+}-H^{\delta+}$ and $X^{\delta-}-Y^{\delta-}$ interactions will destabilize the adduct with respect to M−Y bond dissociation (Figure 1c).

The total energy of the complex formation is divided between electrostatic and covalent contributions in the model of Vogel and Drago.[55] We tentatively assume that this partitioning is valid for MX_3YH_3 systems as well. For a qualitative estimate of the Coulomb and the covalent contributions to the donor−acceptor bond energy, we used the following scheme. The electrostatic (Coulomb) interaction (E_E) was computed as the sum of all coupled interactions, affecting the donor−acceptor bond strength:

$$E_E \rightleftharpoons E_{MY} + 3E_{MH} + 3E_{XY} + 6E_{XH} + 3E'_{XH}$$

The energy of interaction between each pair of point charges may be calculated as $E_{q_1,q_2} = 1391.5q_1q_2/r$ kJ mol^{-1},[56] where r is the distance between point charges q_1 and q_2. The effective charges obtained from the Mulliken population analyses were used as the point charges of each atom in the above equations. The covalent contribution to the energy, E_C, was calculated as the difference between the theoretical formation enthalpy of the adduct and the electrostatic contribution:

$$E_C = \Delta H^{form}_{(298)} - E_E$$

Values obtained for some aluminum complexes are presented in Table 9. Of course, using the effective charges from the Mulliken population analysis is somewhat arbitrary, but we discuss only the trends found, and all presented data are used only for a qualitative description.

From the data in Table 9 one can clearly see a difference between ammonia and other donors. Whereas for NH_3 complexes the electrostatic and the covalent contributions are of the same order, the electrostatic contribution approaches zero for PH_3 and AsH_3. Hence, the dissociation energies of ammonia adducts are about twice as large as those of PH_3 and AsH_3 complexes. Similarly, Jonas et al.[3] found that the $AlCl_3NMe_3$ complex is formed predominantly due to electrostatic interactions and concluded that changing H in $AlCl_3NH_3$ to methyl also leads to a high electrostatic contribution to the dissociation energy.

The total electrostatic interaction of H and X atoms is significant (see Table 9) and may reduce the barrier for internal rotation in adducts as mentioned earlier. The Coulomb H···X interaction will try to minimize the H−X distance and stabilize the eclipsed conformation, resulting in small rotation barriers. In fact, for some complexes, e.g., InF_3NH_3 and GaF_3NH_3, the eclipsed conformations are lower in energy than the staggered structures.

Gallium has the lowest effective charge in the series Al, Ga, and In (in agreement with the higher ionization potential of the Ga atom), and hosts more transferred charge than the Al and In centers. This lowers the electrostatic contribution to the dissociation energies of gallium-containing complexes. Thus, the dissociation energies of the MX_3YH_3 complexes change nonmonotonically: Al > Ga < In.

III. Adducts MX_3PX_3 (M = Al, Ga, In; X = F, Cl, Br, I). If the electrostatic model is suitable for the description of donor−acceptor complexes, then the substitution of a hydrogen atom in the donor molecule by a halogen should greatly decrease the possibility of the complex formation in MX_3-YX_3 systems. In agreement with the electrostatic model, it has been shown experimentally that AlX_3-YX_3 systems are eutectic.[57] In GaX_3-YX_3 systems a 1:1 compound is formed,[58] which melts incongruently (Y = P, As; X = Cl, Br).

However, for the $AlBr_3PBr_3$ complex our electrostatic model is not in agreement with experiment. Whereas the dissociation energy obtained for $AlBr_3PH_3$ at the B3LYP/LANL2DZP level is 58 kJ mol^{-1}, a higher (instead of a lower) dissociation energy of 92.6 kJ mol^{-1} was derived for the $AlBr_3PBr_3$ complex in a gas-phase tensimetric study.[57,59] To solve this discrepancy between the electrostatic model of complex formation and the experimental data, ab initio and B3LYP investigations of MX_3-PX_3 complexes have been carried out.

A staggered ("ethane-like") geometry, with a donor−acceptor single bond, X_3MYX_3, as well as the structure $X_2MX_2YX_2$ with two bridging halogen atoms are usually considered for MX_3-YX_3 systems. Direct electron diffraction data revealed a staggered structure for $AlBr_3SbBr_3$.[60] Note that in the solid state an ionic structure, $SbBr_2^+AlBr_4^-$, is preferred.[61] According to semiempirical data, the substitution of Sb with P increases the stability of the ethane-like structure.[58,62] We find that the bridged $GaCl_3PCl_3$ geometry corresponds to a second-order stationary point which is 170 kJ mol^{-1} higher in energy than the staggered minimum. Hence, the staggered geometries were used in our study of MX_3PX_3 compounds throughout, and vibrational frequency analyses reveal that all ethane-like MX_3PX_3 structures studied are minima.

Theoretical dissociation energies are presented in Figure 8. All trends discussed earlier for MX_3YH_3 systems remain valid. Calculated $\Delta H^{diss}_{(298)}$ values for PX_3 adducts are much lower than for PH_3 adducts, in agreement with the expected trend.

(55) Vogel, G. S.; Drago, R. S. *J. Chem. Educ.* **1996**, *73*, 701.
(56) Clementi, E. *Lect. Notes Chem.* **1980**, *19*, 1.
(57) Suvorov, A. V.; Malkova, A. S.; Avrorina, V. I. *Zh. Neorg. Khim.* **1969**, *14*, 1374.
(58) Volkova, M. V.; Sevastjanova, T. N.; Semenov, S. G.; Suvorov, A. V.; Tarasova, A. S. *Koord. Khim.* **1986**, *12*, 1490.
(59) Malkova, A. S. Ph.D. Thesis, Moscow State University, 1969.
(60) Malkova, A. S.; Spiridonov. *Zh. Neorg. Khim.* **1969**, *14*, 1374.
(61) Coleman, A. P.; Nieuwenhuyzen, M.; Rutt, H. N.; R., S. K. *J. Chem. Soc., Chem. Commun.* **1995**, 2369.
(62) Semenov, S. G.; Suvorov, A. V. *Koord. Khim.* **1977**, *3*, 1823.

Table 10. Theoretical and Experimental Results for MX_4^- Ions and $\Delta H^\circ_{(298)}$ and $\Delta S^\circ_{(298)}$ for the Process $MX_3 + X^- \rightleftharpoons MX_4^-$ in the Gas Phase[a]

							vibrational frequencies and infrared intensities[b]			
MX_4^-	method	R_{M-X}	$S^\circ_{(298)}$	$\Delta H^\circ_{(298)}$	$\Delta S^\circ_{(298)}$	q_{CT}	E	T_2	A_1	T_2
AlF_4^-	SCF/LANL2DZP	1.676	292.9	−559	−127.5	0.328	212	328 (57)	644	826 (250)
	B3LYP/LANL2DZP	1.693	295.6	−570	−135.7	0.409	201	310 (43)	615	791 (198)
	exptl	1.69		−500 ± 13			210	322	622	760
GaF_4^-	SCF/LANL2DZP	1.714	305.0	−536	−126.3	0.289	197	277 (68)	621	641 (119)
	B3LYP/LANL2DZP	1.740	309.2	−548	−125.1	0.410	185	258 (50)	577	602 (97)
	exptl									
InF_4^-	SCF/LANL2DZP	1.854	321.2	−527	−123.1	0.224	161	220 (81)	559	544 (95)
	B3LYP/LANL2DZP	1.878	326.0	−535	−121.7	0.337	147	204 (62)	520	511 (80)
	exptl									
$AlCl_4^-$	SCF/LANL2DZP	2.156	341.5	−368	−121.4	0.481	124	192 (11)	356	519 (215)
	B3LYP/LANL2DZP	2.168	345.7	−375	−128.8	0.532	114	179 (8)	336	498 (179)
	exptl	2.16		−347 ± 29			119	182	348	498
$GaCl_4^-$	SCF/LANL2DZP	2.207	356.4	−343	−118.8	0.577	113	162 (17)	339	374 (108)
	B3LYP/LANL2DZP	2.223	361.4	−352	−117.4	0.621	103	149 (12)	316	358 (92)
	exptl			−334 ± 13			120	153	343	370
$InCl_4^-$	SCF/LANL2DZP	2.364	372.0	−366	−116.5	0.494	93	129 (24)	317	330 (81)
	B3LYP/LANL2DZP	2.385	377.3	−371	−115.0	0.542	85	119 (18)	295	314 (71)
	exptl						89	112	321	337
$AlBr_4^-$	SCF/LANL2DZP	2.353	391.2	−294	−117.9	0.466	72	117 (1)	210	408 (159)
	B3LYP/LANL2DZP	2.364	396.0	−297	−116.1	0.492	66	108 (1)	197	391 (34)
	exptl						98	114	212	394
$GaBr_4^-$	SCF/LANL2DZP	2.394	405.8	−272	−115.0	0.555	67	104 (3)	202	273 (78)
	B3LYP/LANL2DZP	2.411	411.5	−277	−113.1	0.574	60	95 (2)	187	260 (66)
	exptl						71	102	210	278
$InBr_4^-$	SCF/LANL2DZP	2.546	420.6	−297	−113.0	0.489	56	85 (5)	191	229 (58)
	B3LYP/LANL2DZP	2.566	426.8	−297	−110.8	0.515	50	77 (4)	177	218 (50)
	exptl						55	79	197	239
AlI_4^-	SCF/LANL2DZP	2.582	425.3	−228	−114.7	0.489	52	83 (0.2)	145	341 (130)
	B3LYP/LANL2DZP	2.590	430.0	−234	−113.2	0.498	47	77 (0.1)	136	328 (110)
	exptl						51	82	146	336
GaI_4^-	SCF/LANL2DZP	2.614	439.6	−211	−112.4	0.614	48	75 (0.6)	141	223 (65)
	B3LYP/LANL2DZP	2.629	445.3	−218	−110.3	0.616	43	69 (0.3)	130	212 (54)
	exptl						52	73	145	222
InI_4^-	SCF/LANL2DZP	2.765	454.4	−234	−110.1	0.543	40	62 (2)	134	183 (48)
	B3LYP/LANL2DZP	2.783	460.5	−238	−108.2	0.557	36	57 (1)	123	174 (40)
	exptl						42	58	139	185

[a] All distances in Å, angles in deg, entropies in J K^{-1} mol^{-1}, enthalpies in kJ mol^{-1}, vibrational frequencies in cm^{-1}, and infrared intensities (in parentheses) in km mol^{-1}. [b] E and A_1 modes are inactive in the IR spectrum, and their IR intensities are zero.

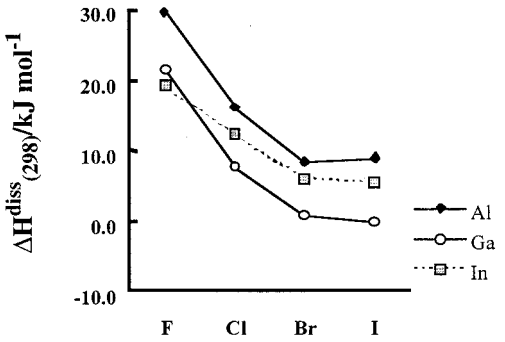

Figure 8. Theoretical dissociation enthalpies, $\Delta H^{diss}_{(298)}$ (kJ mol^{-1}) for MX_3PX_3 complexes.

The largest dissociation energy (30 kJ mol^{-1}) is obtained for AlF_3PF_3, but it is only 10 kJ mol^{-1} for the $AlBr_3PBr_3$ complex, in stark contrast to the 92 kJ mol^{-1} reported experimentally.[57,59]

Note that the experimentally derived dissociation energy, 92 kJ mol^{-1}, is even higher than the Al_2Br_6 dissociation energy, 55.6 kJ mol^{-1}.[2] If the reported value for $AlBr_3PBr_3$ is correct, then the intermolecular interactions of monomeric $AlBr_3$ and PBr_3 should be almost twice as much as the intramolecular interaction of two $AlBr_3$ moieties in the dimer. Therefore, $AlBr_3$-PBr_3 should also exist in the solid state. However, no complexes have been observed in the solid state as the $AlBr_3-PBr_3$ system is eutectic.[57] The analysis of the full set of experimental data available[59] suggests that there is an ambiguity in the experimental assignment of the unsaturated vapor pressure range. The conclusions drawn by the experimentalists about the stability of the $AlBr_3-PBr_3$ complex arise from the wrong assignment of the temperature at which the system became homogeneous.[57,59] Investigation of the $GaCl_3-PCl_3$ system, employing the same experimental techniques, revealed a similar problem;[58] however, in this case the authors correctly concluded that the complex $GaCl_3PCl_3$ does not exist in the vapor phase, in agreement with our theoretical predictions.

IV. MX_3-X^- Systems (M = Al, Ga, In; X = F, Cl, Br, I). Group 13 metal halides MX_3 are well-known catalysts in Friedel−Crafts reactions. Their interaction with halogenohydrides generates the superacids HMX_4. According to a common point of view, metal halides form highly stable anions MX_4^- in Friedel−Crafts reactions, which facilitate the generation of R^+ and RO^+ cations.

$$MX_3 + RX \rightleftharpoons MX_4^- + R^+ \quad \text{or}$$

$$MX_3 + ROX \rightleftharpoons MX_4^- + RO^+$$

However, if some O-, N-, or P-donor molecules are present in the reaction media, then the complex formation with a neutral donor D (1) can compete with anion formation (2).

$$MX_3 + D \rightleftharpoons MX_3D \quad (1)$$

$$MX_3 + X^- \rightleftharpoons MX_4^- \quad (2)$$

Despite the fact that MX_4^- anions have been the subject of experimental investigations in nonaqueous solutions and in the solid state, e.g., $Na^+MX_4^-$,[63,64] their gas-phase structural and thermodynamic properties have not been investigated, with the exception of the fluorine systems.[65,66]

Here we present SCF and B3LYP results for the MX_4^- species (Table 10). The total charge transfer, X^- affinity (i.e., the dissociation energy $MX_4^- \rightarrow MX_3 + X^-$), and charge redistribution on X and M centers are presented in Figure 9a−d. The transferred charge is mostly localized on the halogen atoms. The total charge transfer is much greater and the dissociation energy (X^- affinity) is higher than the corresponding parameters in neutral MX_3YH_3 systems. The computed dissociation energies are 6−14% higher than experimental values (Table 10). This may be attributed to the inadequate description of the X^- anions at the level of theory employed in our computations, as the correct X^- description is a problem for DFT methods. The error in the electron affinities of X is about 0.5 eV, even with extended basis sets.[67] However, since such overestimations are observed for all halides, the trends, derived from the data obtained, should not be affected. Vibrational frequencies of MX_4^- anions are in good agreement with experimental data.[38]

MX_4^- anion formation increases the M−X distances (compared to MX_3), due to the negative charge of the system and possibly also due to the breaking of π interaction in MX_3. It is interesting that the calculated X^- affinity (E_A) of MX_3 correlates linearly with the M−X bond length difference, $\Delta R_{M-X} = R_{M-X}(MX_4^-) - R_{M-X}(MX_3)$ (Figure 10):

$$E_A = -6600\Delta R + 960 \text{ (correlation coefficient 0.990)}$$

The change in the vibrational frequency ν_1, $\Delta\nu_1 = \nu_1(A_1')(MX_3) - \nu_1(A_1)(MX_4^-)$, which corresponds to the M−X bond stretching mode, also correlates with the dissociation energy:

$$E_A = -951\Delta\nu_1 + 125 \text{ (correlation coefficient 0.938)}$$

As mentioned in a recent review on the properties of the halides of group 13 metals,[41] correlations among structural, thermodynamic, and vibrational properties are usually valid for a single central atom only. The linear dependencies $E_A = f(\Delta R)$ and $E_A = f(\Delta\nu_1)$ reported here apply to all tetrahalo anions of Al, Ga, and In. This correlation agrees well with the dependence of the boron−fluorine distance on the dissociation energy of the donor−acceptor bond with a series of donors.[3] The data presented in this work suggest that these correlations have a common origin for all group 13 metal halides.

Conclusions

I. Bond Length and Bond Angle Trends. The B3LYP method slightly increases the bond distances compared to SCF theory and gives good values for valence angles. The Y−H bond lengths in the complexes are essentially constant for each Y (1.006 ± 0.002 Å for ammonia, 1.394 ± 0.002 Å for phosphine, and 1.495 ± 0.002 Å for arsine at the SCF/LANLDZP level) and *do not depend* on the nature of M and X. Changes in the Y−H bond lengths relative to the free donors are only 0.1%. The P−H and As−H distances decrease more significantly than do the N−H bond lengths.

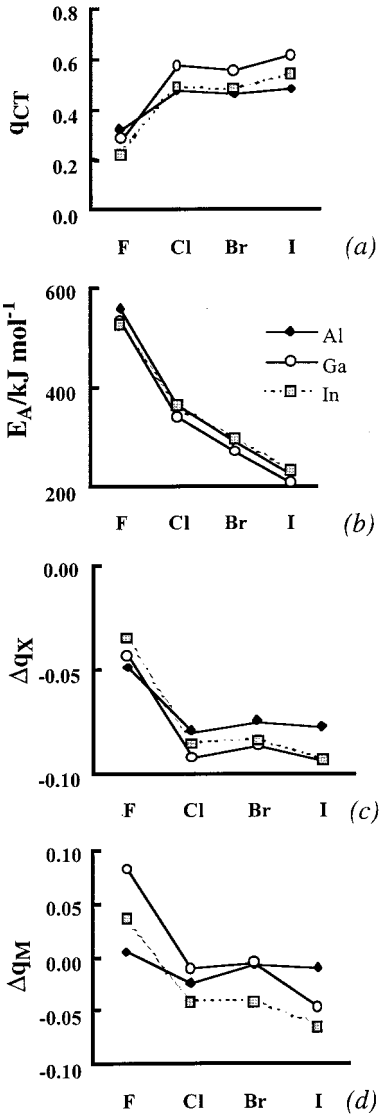

Figure 9. Theoretical characteristics for MH_4^- ions: (a) total charge transfer, (b) X^- affinity, E_A (kJ mol[3]), (c) the change of the effective charge on the X atom, $\Delta q_X = q_X(MX_4^-) - q_X(MX_3)$, (d) the change of the effective charge on the M atom, $\Delta q_M = q_M(MX_4^-) - q_M(MX_3)$.

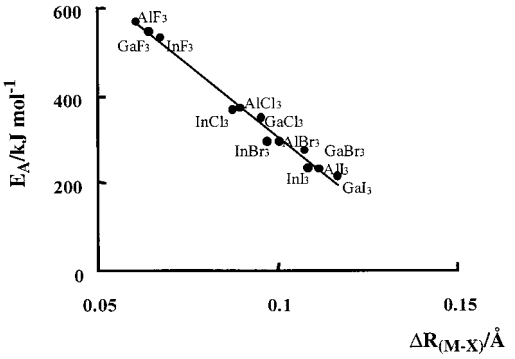

Figure 10. Halogen anion affinity, E_A, vs M−X bond length increase.

(63) Blander, M.; Bierwagen, E.; Calkins, K. G.; Curtiss, L. A.; Price, D. L.; Saboungi, M.-L. *J. Chem. Phys.* **1992**, *97*, 2733.
(64) Bock, C. W.; Trachtman, M.; Mains, G. J. *J. Phys. Chem.* **1994**, *98*, 8.
(65) Gutsev, G.; Les, A.; Adamowicz, L. *J. Chem. Phys.* **1994**, *100*, 8925.
(66) Bouyer, F.; Picard, G.; Legendre, J.-J. *Int. J. Quantum Chem.* **1994**, *52*, 927.
(67) Gailbraigh, J. M.; Schaefer, H. F. *J. Chem. Phys.* **1996**, *105*, 682.

Compared to the free acceptors, the M−X distances in the adducts increase by 0.02 Å for fluorides to 0.05 Å for iodides. These changes are much smaller than those found for boron halides, where the B−Cl distances increase by 0.1 Å compared to free BCl_3.[3] Due to the interaction with the donor YH_3, the X−M−Y angle increases with respect to separated MX_3 and YH_3 species. Since the energy needed to elongate the bond is much larger than that for angle deformation,[39] it is not surprising that the relative bond length increase is 10 times less than the X−M−Y angle deformation.

A similar relationship between bond angle widening and bond lengthening was found by Mastryukov and Schapin for some hydrocarbons,[68] and studied in detail by Shirley et al. for CX_4, CXH_3, and CHX_3 (X = H, Cl, F),[69] as well as by Mota et al. for M_2X_8 and $M_2X_8L_2$ systems with triple and quadruple metal−metal bonds.[70] In the latter study, the M−M−X angle and the M−M bond distance were found to correlate with a correlation coefficient of 0.998 for each metal center (M = Cr, Mo, W).[70]

The M−X bond lengths do not significantly depend on the nature of the donor and remain constant within ±0.002 Å for each M, X pair. This fact illustrates the difference in behavior between boron and other group 13 elements. It was found for BF_3 adducts that the B−F distance in the complex strongly depends on the dissociation energy of the complex.[3] In the present work we obtained almost the same M−X bond lengths for the strongly and weakly bonded adducts. This invariance of the M−X distance for Al, Ga, and In halides indicates that donation of electron density to the central atom becomes less important when the atomic radius of the central atom is large.

Accompanied by the small M−X bond length increase is the distortion of the acceptor molecule from planarity during complex formation, which reduces the X−M−X and X−M−Y angles, although changes of the latter are more obvious: this angle ranges from 90° (when the noninteracting donor is aligned along the 3-fold symmetry axis of the acceptor species) up to 109.5° in MX_4^-. There is a correlation between the *relative* bond length increase, $\Delta R_{M-X}/R_{M-X}(MX_3)$, where $\Delta R_{M-X} = R_{M-X}(MX_3D) - R_{M-X}(MX_3)$ and *relative* increase of the X−M−Y angle, $\Delta\alpha_{X-M-Y}/90$, $\Delta\alpha_{X-M-Y} = \alpha_{X-M-Y}(MX_3D) - 90.0$. Note that this correlation (correlation coefficient 0.9735) is observed for all 60 investigated species MX_3YH_3, MX_3PX_3, and MX_4^- (Figure 11).

$$\Delta R_{M-X}/R_{M-X}(MX_3) = 2.122\Delta\alpha_{X-M-Y}/90 - 0.0045$$

In Figure 4, the theoretical donor−acceptor distances for MX_3YH_3 adducts are presented. The M−N distances are in good agreement with gas-phase experimental data; the M−N distance slightly increases from Cl to I, whereas it is roughly the same for the fluoride and chloride complexes.

Using the X−M−Y pyramidalization angle and the M−Y bond length, we get a linear correlation for each YH_3 used; however, the correlation coefficients are not very high (0.8−0.97). This is mostly due to specific charge redistribution of the fluorine systems, mentioned above. The short M−F distances and the high negative effective charges lead to unfavorable distortions in the fluorine systems. When fluorine systems are excluded, there is a nearly perfect correlation between the X−M−Y angle and the M−Y distance with correlation coefficient 0.99 for each of the donors (NH_3, PH_3, AsH_3) (Figure 12). The fact that a correlation exists for each donor separately may arise from electrostatic interactions. Indeed, for negatively charged nitrogen, the bond length M−N is the shortest (electrostatic stabilization of $M^{\delta+}\cdots N^{\delta-}$) and the X−M−Y angle is the largest (large destabilization $X^{\delta-}\cdots N^{\delta-}$). Substituting nitrogen with P and As, which have low effective charges, decreases the X−M−Y angle and leads to longer M−Y bonds.

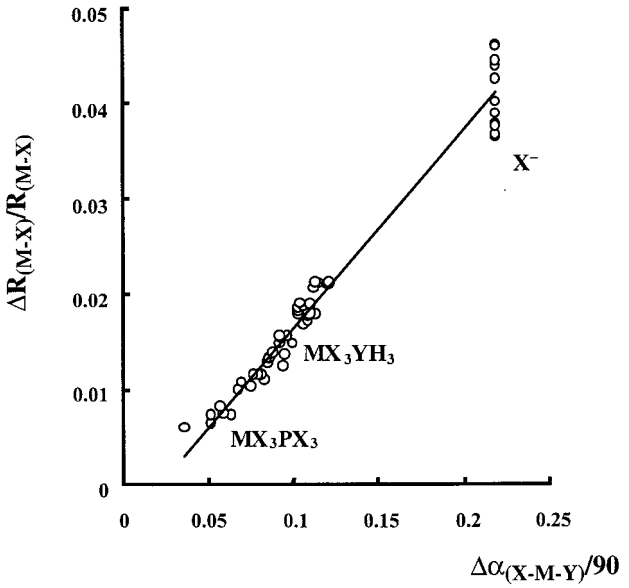

Figure 11. Relative bond length increase R_{M-X}/R_{M-X} vs relative X−M−Y angle increase $\alpha_{X-M-Y}/90$.

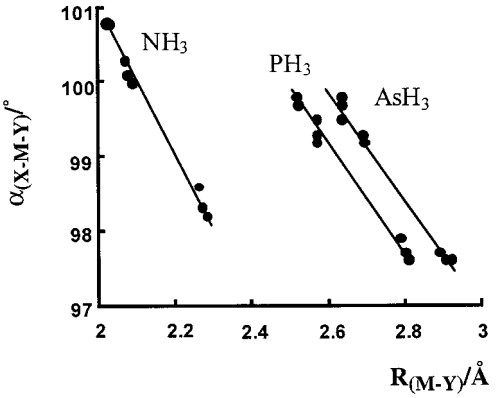

Figure 12. Bond length−bond angle relationship for MX_3YH_3 systems.

For the MX_4^- case, the tetrahedral angle X−M−Y stays the same for all metal halides, and the relative M−X bond length increase is constant to within 4.2%, despite the huge bond energy differences, ranging from 220 to 570 kJ mol^{-1}.

II. Vibrational Frequency Trends. The B3LYP method gives good results for the vibrational frequencies of all classes of inorganic compounds that were investigated in the present work. Experimental and B3LYP vibrational frequencies for organic molecules have been compared, and a selective scaling procedure has been proposed by Rauhut and Pulay.[71] It was found for a small number of inorganic compounds that B3LYP overestimates vibrational frequencies above 500 cm^{-1}, but underestimates frequencies under 500 cm^{-1}.[44] In the present study we obtained a good correlation between observed and theoretical vibration frequencies for MX_3 metal halides, donor molecules YH_3, and ions MX_4^-. The full set of vibrational frequencies gives a satisfying agreement between computed and

(68) Mastryukov, V. S.; Schapin, I. Y. *Vestn. MGU, Ser. Khim.* **1991**, *32*, 569.

(69) Shirley, W. A.; Hoffmann, R.; Mastryukov, V. S. *J. Phys. Chem.* **1995**, *99*, 4025.

(70) Mota, F.; Novoa, J. J.; Losada, J.; Alvarez, S.; Hoffmann, R.; Silvestre, J. *J. Am. Chem. Soc.* **1993**, *115*, 6216.

(71) Rauhut, G.; Pulay, P. *J. Phys. Chem.* **1995**, *99*, 3093.

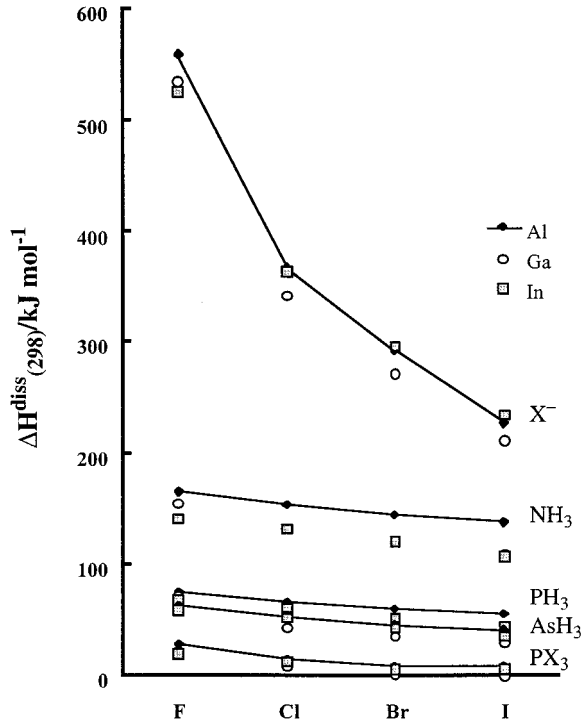

Figure 13. Dissociation enthalpies $\Delta H^{diss}_{(298)}$ (kJ mol^{-1}) for all investigated compounds.

observed values, $\nu_{obsd} = 0.9578\omega_{calcd} + 12.885$, with a regression coefficient of 0.9988. The underestimation of vibrational frequencies below 500 cm^{-1} is found only for donor molecules. B3LYP vibrational frequencies in the range up to 1000 cm^{-1} are both lower and higher than experimental vibrational frequencies for the metal halides.

III. Donor and Acceptor Strength Order. Comparing the theoretical predictions for all systems, we conclude that in complexes between MX_3 and YX_3 the electrostatic interaction plays a significant role. The dissociation enthalpies for all complexes are given in Figure 13. The electrostatic contribution to the dissociation energies is similar in size to the covalent contribution in complexes involving X^- and NH_3, but it is less important for PH_3 and AsH_3 containing adducts. Hence, the latter systems have lower dissociation energies. The instability of MX_3PX_3 systems in the gas phase and in the solid state is due to the destabilizing electrostatic interaction.

Our work suggests that there is no simple correlation between the amount of charge transfer and the bond strength in the donor−acceptor complexes MX_3-YH_3. Ammonia adducts have mostly ionic metal−donor bonds, while adducts with phosphine and arsine are mostly covalently bound.

Entropy destabilizes the donor−acceptor complexes by 30−40 kJ mol^{-1} at room temperature. Whereas adducts of ammonia are stable in the gas phase (at 298 K), the PH_3, PX_3, and AsH_3 complexes are unstable. With the data for metal hydrides derived by Jungwirth and Zahradnik,[17] we obtain the following sequence of acceptor abilities for metal (Al, Ga, In) halides with ammonia:

$$F > Cl > Br > I > H$$

Our results agree well with the order established for water adducts by Frenking and co-workers.[22] This order is different from that of the acceptor strength of boron halides, which is F < Cl < H.[8,22] Jungwirth and Zahradnik[17] found the complexes of phosphine with metal hydrides to be unstable. Our results indicate that phosphine complexes with Al, Ga, and In halides are more stable under normal conditions than the analogous hydride compounds.

Hirota et al. pointed out that the experimental sequence of the acceptor strength of boron halides agrees much better with the calculated charge-transfer q_{CT} than with the calculated dissociation energy.[8] This is not true for metal halide systems, where the electrostatic contribution to the dissociation energy can be significant. As was shown by Jonas et al.,[3] the strong complex $BCl_3-N(CH_3)_3$ is formed mostly by covalent interactions, while the strong $AlCl_3-N(CH_3)_3$ complex has an ionic nature.

Taking into account all theoretical data on the stability of MX_3D systems, we emphasize that the acceptor strength of metal halides decreases in the orders F > Cl > Br > I and Al > Ga < In *for all donors investigated* and that the donor strength follows the order $X^- > NH_3 > H_2O > PH_3 > AsH_3 > PX_3$ for all Al, Ga, and In halides.

Acknowledgment. This research was supported by the U.S. National Science Foundation, Grant CHE-9527468. A.Y.T. gratefully acknowledges support from the Grant Center for Natural Sciences, Grant No. M97-2.3K-697.

Supporting Information Available: A full set of structural and thermodynamic properties of all 36 distinct complexes (PDF). This material is available free of charge via the Internet at http://pubs.acs.org.

JA983408T